
[View Journal Online](#)  
[View Article Online](#)

# Synthesis, characterization and Hirshfeld surface analysis of 2-aminobenzothiazol with 4-fluorobenzoic acid co-crystal

 Bubun Banerjee <sup>1</sup>, Varun Sharma <sup>2</sup>, Aditi Sharma <sup>1</sup>,  
 Gurpreet Kaur <sup>1</sup> and Vivek Kumar Gupta <sup>2,\*</sup>
<sup>1</sup> Department of Chemistry, Akal University, Talwandi Sabo, Bathinda, Punjab-151302, India<sup>2</sup> Department of Physics, University of Jammu, Jammu Tawi-180006, India\* Corresponding author at: Department of Physics, University of Jammu, Jammu Tawi-180006, India.  
 e-mail: [vivek.gupta2k9@gmail.com](mailto:vivek.gupta2k9@gmail.com) (V.K. Gupta).

## RESEARCH ARTICLE

## ABSTRACT



doi: 10.5155/eurjchem.13.2.206-213.2234

Received: 02 March 2022

Received in revised form: 14 April 2022

Accepted: 26 April 2022

Published online: 30 June 2022

Printed: 30 June 2022

## KEYWORDS

 Co-crystal  
 X-ray diffraction  
 Hirshfeld surface  
 Hydrogen bonding  
 4-Fluorobenzoic acid  
 2-Aminobenzothiazol

The co-crystal of 2-aminobenzothiazol with 4-fluorobenzoic acid were synthesized and characterized by elemental analyses, spectral studies (FT-IR, NMR, HRMS) and single-crystal X-ray diffraction analysis. This compound co-crystallizes in the monoclinic space group  $P2_1/c$  (no. 14),  $a = 11.7869(14)$  Å,  $b = 4.0326(5)$  Å,  $c = 27.625(3)$  Å,  $\beta = 92.731(10)^\circ$ ,  $V = 1311.6(3)$  Å<sup>3</sup>,  $Z = 4$ ,  $T = 293(2)$  K,  $\mu(\text{CuK}\alpha) = 2.345$  mm<sup>-1</sup>,  $D_{\text{calc}} = 1.470$  g/cm<sup>3</sup>, 3568 reflections measured ( $7.508^\circ \leq 2\theta \leq 134.202^\circ$ ), 2280 unique ( $R_{\text{int}} = 0.0262$ ,  $R_{\text{sigma}} = 0.0413$ ) which were used in all calculations. The final  $R_1$  was 0.0446 ( $I > 2\sigma(I)$ ) and  $wR_2$  was 0.1274 (all data). The crystal structure is stabilized by elaborate system of N-H...O and O-H...O hydrogen bonds to form supramolecular structures. Furthermore, the 3D Hirshfeld surfaces and the associated 2D fingerprint plots have been analyzed for molecular interactions.

Cite this: *Eur. J. Chem.* 2022, 13(2), 206-213Journal website: [www.eurjchem.com](http://www.eurjchem.com)

## 1. Introduction

Easy and smooth delivery of the active pharmacological ingredient is one of the important parts of drug development. Most of the cases, the active pharmacological ingredients are crystalline solids at ambient temperature and are generally provided as a tablet form [1]. It is well established that the efficacy of a drug molecule depends on its physical properties such as dissolution rate, solubility, melting point, color *etc.* which again varies depending upon the packing of its crystal [2]. Co-crystallization offers significant benefit by delivering two or more different active pharmacological ingredients at a time, which in many occasions provides better efficacy than the individual single component [3]. Since the first formation of co-crystal between nucleic bases [4], these were recognized as valuable materials and gained significant attention [5-8]. These were reported to use as pharmaceutical materials [9,10], electronic and optical materials [11,12] and even employed as media for conducting solid-state organic syntheses [13-16].

Benzothiazole (Benzo[d]thiazol) is an important class of fused heterocyclic scaffold having broad range of pharmaceutical applications such as antimicrobial [17], anti-inflammatory [18], anticancer activities [19,20], neuroprotective [21], anti-

helmintic [22], anticonvulsant [23], antigitamate [24], anti-malarial [25], antitubercular [26] and so on. Figure 1 represents a glimpse of drug molecules having benzothiazole as the core skeleton [27].

Very recently, we have reported the X-ray diffraction analysis of a co-crystal formed between 2-aminobenzothiazol and 1-methylisatin [28]. In continuation of our strong interest towards the crystal structure of bioactive organic molecules [29-40], in this communication, we want to report the detailed X-ray diffraction analysis along with FT-IR, NMR, and HRMS studies of another co-crystal (III) formed between 4-fluoro benzoic acid and 2-aminobenzothiazol. We strongly believe that co-crystallization of these two highly active pharmacological ingredients will surely make some impact and show high therapeutic potentials. Screening of biological activities of this co-crystal is under process which will be communicated later on.

## 2. Experimental

## 2.1. General

Infrared spectra were recorded on Agilent (Cary 660) FT-IR spectrophotometer on KBr discs.

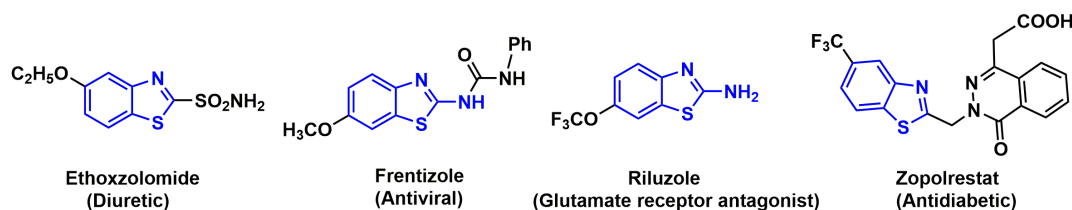
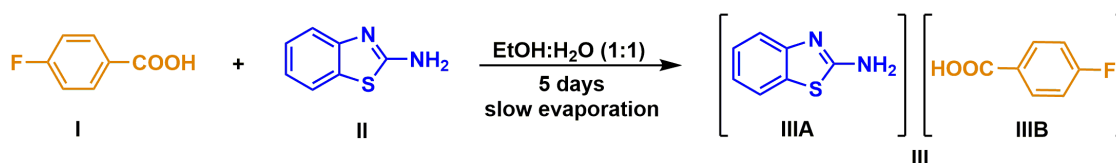


Figure 1. Drug molecules with benzothiazole skeleton.



Scheme 1. Preparation of 1:1 co-crystal of 4-fluorobenzoic and 2-aminobenzothiazol.

$^1\text{H}$  and  $^{13}\text{C}$  NMR spectra were obtained at 500 MHz Jeol (JNM ECX-500) NMR machines with  $\text{CDCl}_3$  as the solvent. Mass spectra (TOF-MS ES+) were measured on a Bruker Impact HD QTOF Micro mass spectrometer. Melting points were recorded on a Digital Melting Point Apparatus (Model No. MT-934) and are uncorrected. TLC was performed on silica gel 60F<sub>254</sub> (Merck) plates. Single crystal data was collected on Agilent Technologies (Oxford Diffraction) Supernova single crystal diffractometer.

## 2.2. Preparation of co-crystal

1:1 Co-crystals of 4-fluorobenzoic acid and 2-amino benzothiazol (**III**, 0.270 g; 0.93 mmol) were obtained from the equimolar mixture of 4-fluorobenzoic acid (**I**, 0.280 g, 2 mmol) and 2-aminobenzothiazol (**II**, 0.301 g, 2 mmol) in aqueous ethanol (1:1, v:v). Slow evaporation of the solution at room temperature resulted in the formation of white block-shaped co-crystals (Scheme 1).

**4-Fluorobenzoic acid (I)**: Color: White powder. FT-IR (KBr,  $\nu$ ,  $\text{cm}^{-1}$ ): 3082, 2987, 2826, 2667, 2552, 1674, 1599, 1509, 1423, 1293, 1224, 1130, 924, 847, 765.  $^1\text{H}$  NMR (500 MHz,  $\text{CDCl}_3$ ,  $\delta$ , ppm): 9.97 (1H, s, OH), 8.14-8.12 (2H, m, Ar-H), 7.15 (2H, t,  $J = 8.50$  Hz, Ar-H).

**2-Aminobenzothiazol (II)**: Color: White powder. FT-IR (KBr,  $\nu$ ,  $\text{cm}^{-1}$ ): 3060, 1716, 1588, 1503, 1420, 1276, 1014, 829.  $^1\text{H}$  NMR (500 MHz,  $\text{CDCl}_3$ ,  $\delta$ , ppm): 7.59 (1H, dd,  $J = 7.92, 1.30, 1.25$  Hz, Ar-H), 7.54 (1H, dd,  $J = 8.05, 1.15$  Hz, Ar-H), 7.31 (1H, td,  $J = 7.33, 1.30, 1.25$  Hz, Ar-H), 7.13 (1H, td,  $J = 7.58, 7.68, 1.20$  Hz, Ar-H), 5.45 (2H, s,  $\text{NH}_2$ ).

**Co-crystal of 2-aminobenzothiazol and 4-fluorobenzoic acid (1:1) (III)**: Color: Colorless crystal. FT-IR (KBr,  $\nu$ ,  $\text{cm}^{-1}$ ): 3401, 3305, 3169, 2358, 1671, 1624, 1600, 1542, 1509, 1453, 1329, 1228 1126, 1091, 854, 744.  $^1\text{H}$  NMR (500 MHz,  $\text{CDCl}_3$ ,  $\delta$ , ppm): 8.15 (2H, dd,  $J = 8.90, 5.5$  Hz, Ar-H), 7.58-7.54 (2H, m, Ar-H), 7.34 (1H, t,  $J = 7.55$  Hz, Ar-H), 7.17-7.12 (3H, m, Ar-H), 6.73 (2H, s,  $\text{NH}_2$ ).  $^{13}\text{C}$  NMR (125 MHz,  $\text{CDCl}_3$ ,  $\delta$ , ppm): 170.33, 168.08, 166.84, 164.83, 149.42, 132.51, 132.44, 129.31, 127.07, 126.35, 122.62, 121.06, 118.01, 115.53, 115.35.

## 2.3. Crystal structure determination and refinement

Single block crystals of the compounds,  $\text{C}_{14}\text{H}_{11}\text{N}_2\text{O}_2\text{S}$  (**III**) with dimensions of  $0.30 \times 0.20 \times 0.20$  mm were used for data collection. X-ray diffraction study was done on Agilent Technologies (Oxford Diffraction) Supernova single crystal diffractometer using radiation ( $\lambda = 1.54184 \text{ \AA}$ ). X-ray intensity data of 3568 reflections were collected at 293(2) K and out of these reflections 2280 were found unique. The intensities were

measured by  $\omega$  scan mode for  $\theta$  ranges  $3.75$  to  $67.10^\circ$ , where 2158 reflections with  $I > 2\sigma(I)$  were treated as observed. Data was corrected for Lorentz-polarization and absorption factors. The molecular structure was solved by direct methods using SHELXT package [41]. Multisolution tangent refinement was used. All non-hydrogen atoms of the molecule were located in the best  $E$ -map and refined in anisotropic approximation using SHELXS [41]. All hydrogen atoms were geometrically fixed and allowed to ride on the corresponding non-H atoms with  $\text{N-H} = 0.86 \text{ \AA}$ ,  $\text{C-H} = 0.93\text{-}0.98 \text{ \AA}$  and  $U_{\text{iso}}(\text{H}) = 1.5 U_{\text{eq}}$  of the attached C atoms for methyl groups and  $1.2 U_{\text{eq}}(\text{N, C})$  for other H atoms. The geometry of the molecule was calculated using the WinGX [42], PARST [43], and PLATON [44] software. The crystallographic data are summarized in Table 1.

## 2.4. Hirshfeld surfaces calculations

In order to carry out the Hirshfeld surface analysis and to create fingerprint plots, Crystal Explorer 17.5 program [45] was used, for which the crystallographic information file (CIF) was used as input. The molecular Hirshfeld surface of compound **III** was generated using a standard (high) surface resolution with the 3D  $d_{\text{norm}}$  surfaces, the shape index and curvature. The surfaces were shown to be transparent to allow visualization of the molecular moiety in a similar orientation for all of the structures around which they were calculated. 2D fingerprint graphs are plotted by accumulating ( $d_i, d_e$ ) pairs.

## 3. Results and discussion

### 3.1. Synthesis

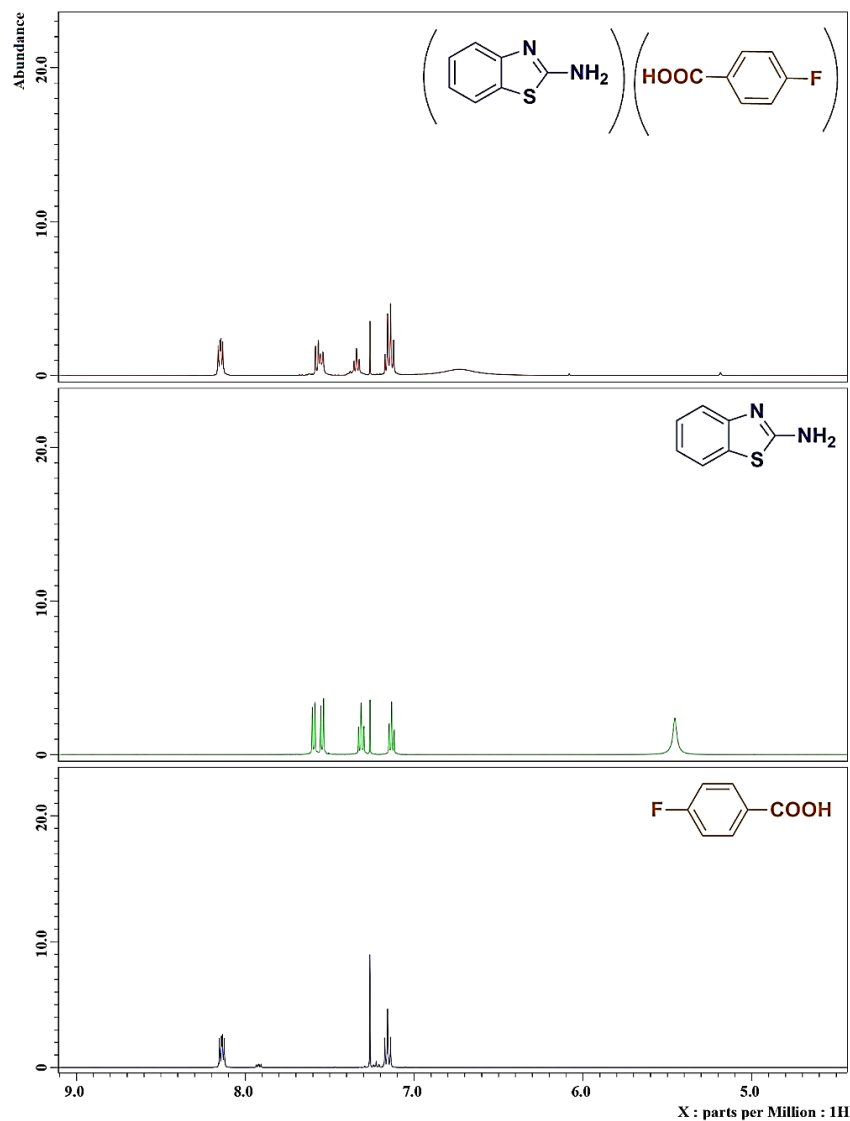
We have compared the  $^1\text{H}$  NMR data of compounds **I**, **II**, and **III** (Figure 2). In the  $^1\text{H}$  NMR spectrum of compound **II**, peak for  $-\text{NH}_2$  appeared at  $\delta_{\text{H}} 5.45$  ppm (2H, s), in this case, a sharp singlet peak was obtained. Whereas a small broad singlet peak was recorded at  $\delta_{\text{H}} 6.73$  ppm (2H, brs) for the same  $-\text{NH}_2$  protons in co-crystal **III**. This little bit higher value indicates there must be some deficiency of electron density over  $-\text{NH}_2$  in the co-crystal **III**, which is definitely due to the formation of strong hydrogen bonds. Other peaks are almost comparable in the individual as well as co-crystal form.

### 3.2. Single crystal X-ray structure analysis

An ORTEP view [46] of the co-crystal **III** with atomic labeling is shown in Figure 3. The bond lengths and angles in the compounds are comparable with literature values [47] and the selected bond distances and angles are shown in Table 2.

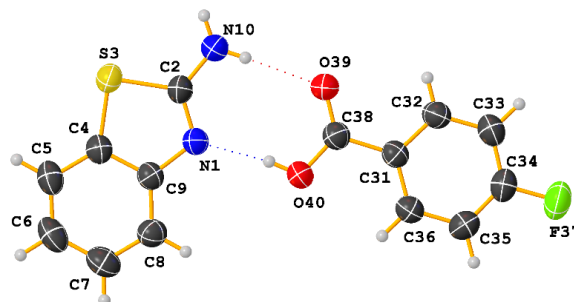
**Table 1.** Crystal data and structure refinement for compound III.

Empirical formula	C <sub>14</sub> H <sub>11</sub> FN <sub>2</sub> O <sub>2</sub> S
Formula weight	290.31
Temperature (K)	293(2)
Crystal system	Monoclinic
Space group	P2 <sub>1</sub> /c
a, (Å)	11.7869(14)
b, (Å)	4.0326(5)
c, (Å)	27.625(3)
α (°)	90
β (°)	92.731(10)
γ (°)	90
Volume (Å <sup>3</sup> )	1311.6(3)
Z	4
ρ <sub>calc</sub> (g/cm <sup>3</sup> )	1.470
μ (mm <sup>-1</sup> )	2.345
F(000)	600.0
Crystal size (mm <sup>3</sup> )	0.3 × 0.2 × 0.2
Radiation	CuKα (λ = 1.54184)
2θ range for data collection (°)	7.508 to 134.202
Index ranges	-13 ≤ h ≤ 14, -3 ≤ k ≤ 4, -28 ≤ l ≤ 32
Reflections collected	3568
Independent reflections	2280 [R <sub>int</sub> = 0.0262, R <sub>sigma</sub> = 0.0413]
Data/restraints/parameters	2280/0/189
Goodness-of-fit on F <sup>2</sup>	1.009
Final R indexes [I ≥ 2σ (I)]	R <sub>1</sub> = 0.0446, wR <sub>2</sub> = 0.1139
Final R indexes [all data]	R <sub>1</sub> = 0.0615, wR <sub>2</sub> = 0.1274
Largest diff. peak/hole (e.Å <sup>-3</sup> )	0.22/-0.28

**Figure 2.** Comparison of <sup>1</sup>H NMR of compounds I, II and co-crystal III.

**Table 2.** Selected bond lengths and angles for compound III.

Atom	Atom	Length (Å)	Atom	Atom	Length (Å)		
S3	C4	1.741(3)	C31	C32	1.383(4)		
S3	C2	1.755(3)	C35	C34	1.367(4)		
F37	C34	1.354(3)	C35	C36	1.376(4)		
O40	C38	1.292(3)	C34	C33	1.373(4)		
C4	C9	1.404(4)	N1	C9	1.385(3)		
C4	C5	1.377(4)	C8	C9	1.389(4)		
O39	C38	1.219(3)	C8	C7	1.374(4)		
C2	N10	1.317(4)	C7	C6	1.391(5)		
C2	N1	1.315(3)	C32	C33	1.378(4)		
C31	C36	1.389(4)	C6	C5	1.378(4)		
C31	C38	1.495(4)					
Atom	Atom	Atom	Angle (°)	Atom	Atom	Atom	Angle (°)
C4	S3	C2	89.29(12)	C2	N1	C9	111.0(2)
C9	C4	S3	109.27(19)	C35	C36	C31	120.9(3)
C5	C4	S3	128.7(2)	O40	C38	C31	115.4(2)
C5	C4	C9	122.0(3)	O39	C38	O40	124.0(3)
N10	C2	S3	120.9(2)	O39	C38	C31	120.6(2)
N1	C2	S3	115.12(19)	C7	C8	C9	119.1(3)
N1	C2	N10	124.0(3)	N1	C9	C4	115.3(2)
C36	C31	C38	121.9(2)	N1	C9	C8	125.7(2)
C32	C31	C36	119.1(3)	C8	C9	C4	119.0(2)
C32	C31	C38	119.0(2)	C8	C7	C6	121.1(3)
C34	C35	C36	118.2(3)	C33	C32	C31	120.7(3)
F37	C34	C35	119.0(3)	C5	C6	C7	120.9(3)
F37	C34	C33	118.2(3)	C4	C5	C6	117.9(3)
C35	C34	C33	122.8(3)	C34	C33	C32	118.3(3)

**Figure 3.** The structure of the co-crystal (III), displacement ellipsoids are drawn at 50% probability level.

The X-ray diffraction analyses showed that asymmetric unit of co-crystal of compound III consisted of two crystallographically independent molecules one of 2-aminobenzothiazol IIIA and other of 4-fluorobenzoic IIIB. The geometrical parameters of 2-aminobenzothiazol moiety shows slightly different and are in good agreement with those of related co-crystal structure (C<sub>14</sub>H<sub>10</sub>BrN<sub>3</sub>O<sub>4</sub>S) [48].

The double bond character of the N1-C2 is confirmed by its distance of 1.315(3) Å (IIIA). The S3-C4 = 1.741(3) Å, S3-C2 = 1.755(3) Å (IIIA) exhibit small variations from the reported for values of 1.764 Å, 1.741 Å for related co-crystal (C<sub>14</sub>H<sub>10</sub>BrN<sub>3</sub>O<sub>4</sub>S) [48], these differences may be due to ring strain and electron delocalization. In addition, the bond distance of 1.317(4) Å for C2-N10 shows variation from its reported value of 1.342 Å in similar co-crystal (C<sub>14</sub>H<sub>10</sub>BrN<sub>3</sub>O<sub>4</sub>S) [48]. The bond angles C9-N1-C2 = 111.0(2)°, N1-C2-S3 = 115.12(19)° and C2-S3-C4 = 89.29(12)° of 2-aminobenzothiazol moiety (IIIA) is found to be comparable [110.26°, 115.97°, 88.69°] with the value of the reported co-crystal (C<sub>14</sub>H<sub>10</sub>BrN<sub>3</sub>O<sub>4</sub>S) [48].

In 4-fluorobenzoic acid moiety (IIIB), the bond distance the double bond C38-O39 = 1.219(3) Å and single bond C38-O40 = 1.292(3) Å shows variation from [1.251 Å, 1.282 Å] with the reported co-crystal (C<sub>7</sub>H<sub>5</sub>O<sub>2</sub>F) [49]. In the benzene rings systems, the endocyclic angles at C5, C33, C34 and C35 are narrowed while those at C4 and C7 are expanded from 120°, respectively.

The substituted group makes torsion angles N10-C2-N1-C9 = -179.4(3)° (IIIA), C38-C31-C32-C33 = -179.2(3)° (IIIB) with the respective moieties. All rings of compound III are planar in conformation with maximum deviation for C1 [0.024(3)] of 2-aminobenzothiazol ring, and for C32 [0.007(3)] of benzene ring.

The dihedral angle between aminobenzothiazol and fluoro-benzoic acid moieties of 170.78(8)° shows that both the moieties are to equatorial to each other.

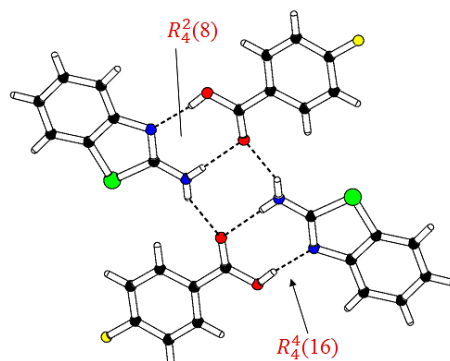
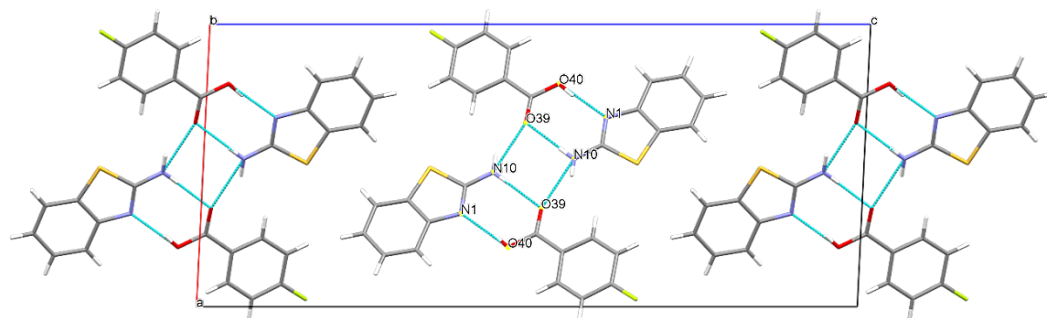
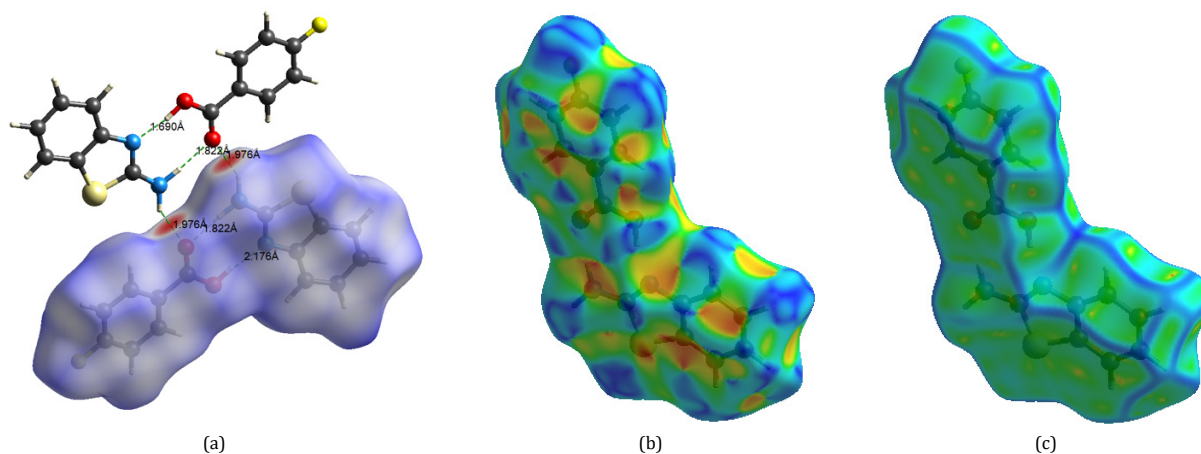
Hydrogen bonding is one of the most important non-covalent interactions that can determine and control the assembly of molecules and ions. Analysis of the crystal packing showed only intermolecular hydrogen bonds in compound III. Both the active H atoms of the NH<sub>2</sub> group participate in intermolecular N-H...O type hydrogen bonds in compound III. In this co-crystal structure, the molecules are linked by a pair of N10-H102...O39 and O40-H401...N1 hydrogen bonds with inversion dimmers forming R<sub>4</sub><sup>2</sup>(8) and R<sub>4</sub><sup>4</sup>(16) ring motifs [50] (Figure 4). These dimmers are further connected by another hydrogen bond N10-H101...O39 in a two-dimensional network, thus forming layer shaped structures along *b*-axis (Figure 5). The best packing view for compounds III is obtained along *b*-axis. Details about all interactions are given in Table 3.

### 3.3. Hirshfeld surface analysis

For obtaining additional insight into the intermolecular interaction of molecular crystals, the Hirshfeld surface is a suitable tool for qualitative and quantitative study and mapping of intermolecular close contacts in molecular crystals. Figure 6 shows the 3D Hirshfeld *d*<sub>norm</sub> surfaces, the shape index and curvature for co-crystal III, which are achieved by mapping *d*<sub>norm</sub> over the Hirshfeld surface in the range from -0.4870 to 1.3305 a.u. for co-crystal III. This indicates interactions between neighboring molecules [51,52].

**Table 3.** Geometry of inter- and intramolecular interactions for compound **III**.

<i>D</i> – <i>H</i> ⋯ <i>A</i>	<i>D</i> – <i>H</i> , Å	<i>H</i> ⋯ <i>A</i> , Å	<i>D</i> ⋯ <i>A</i> , Å	$\theta$ ( <i>D</i> – <i>H</i> ⋯ <i>A</i> ), deg
N10–H101⋯O39 <sup>i</sup>	0.84(4)	2.13(4)	2.883(4)	151(3)
N10–H102⋯O39 <sup>ii</sup>	0.78(4)	2.05(4)	2.830(4)	176(4)
O40–H401⋯N1	0.82	1.85	2.664(3)	171

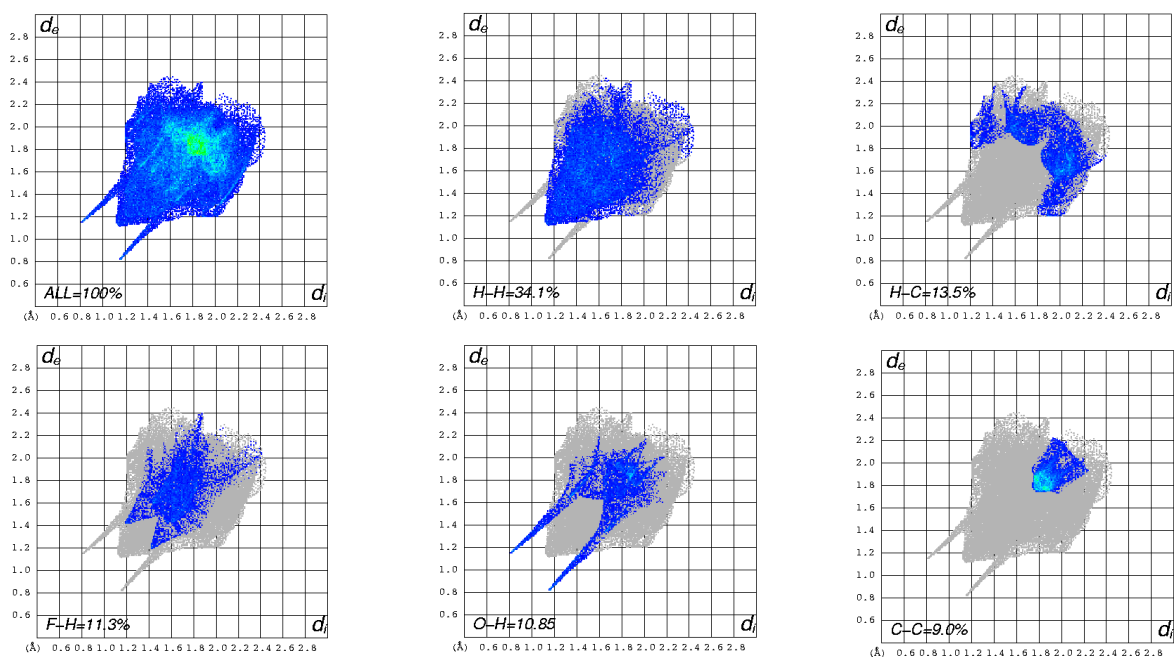
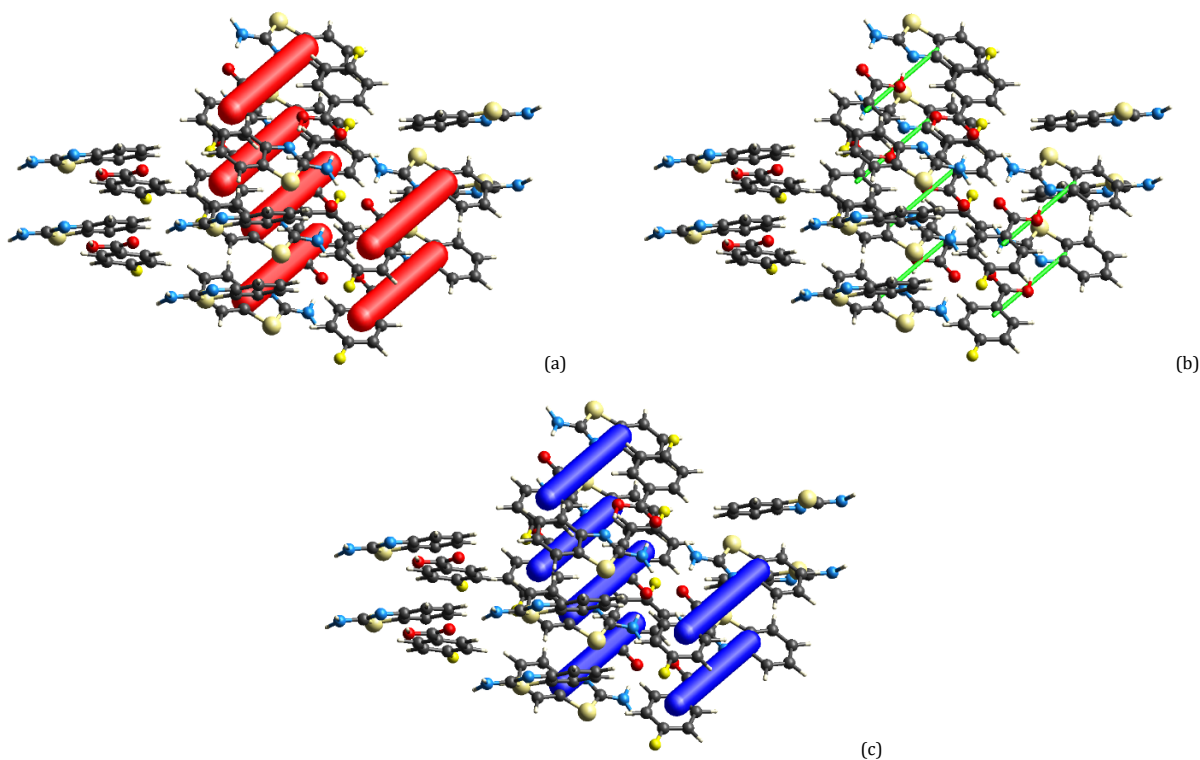
Symmetry codes: (i)  $x, 1+y, z$ ; (ii)  $1-x, 1-y, -z$ .**Figure 4.** A plot of molecules of the co-crystal **III** showing the formation of dimers by intermolecular N–H⋯O and O–H⋯N hydrogen bonds forming  $R_4^2(8)$  and  $R_4^1(16)$  ring motif.**Figure 5.** Packing view of molecules viewed down the *b*-axis within the unit cell of compound **III**.**Figure 6.** Hirshfeld surface: (a)  $d_{norm}$ , (b) shape index, and (c) curvature for co-crystal **III**.

In Figure 6a, we see that the long cyclic hydrogen bond between H102 and O39 is associated with two large red spots of the same size, as identical pair on the surface forming inversion dimers. Figure 6b shows the lack of self-complementary patches of triangles on the shape index surface, which symbolizes a weaker and longer C–H⋯ $\pi$  stacking. Figure 6c displays very small regions of green (relatively flat) separated by dark blue boundaries (large positive curvature), indicating the involvement of any aromatic-aromatic sequence in co-crystal **III**.

The corresponding 2-D fingerprint plots for Hirshfeld surfaces of compound **III** displaying major intermolecular interactions with their percentage of contribution to the total Hirshfeld surface area are shown in Figure 7 along with labeled intermolecular contact values [53]. Table 4 shows that H⋯H interaction following H⋯C/C⋯H interaction with 34.1 and 13.5%, respectively, had a significant contribution among all total Hirshfeld surfaces. The O⋯H/H⋯O intermolecular interactions clearly appear as distinct spikes in the 2D fingerprint.

**Table 4.** Summary of the various intermolecular contacts contributed to the Hirshfeld surface for co-crystal III.

Intermolecular interaction	Contribution (%), >1.0
H...H	34.1
H...C/C...H	13.5
F...H/H...F	11.3
O...H/H...O	10.8
C...C	9.0
H...N/N...H	3.1
F...C/C...F	2.9
S...C/C...S	2.1
O...C/C...O	1.7
C...N/N...C	1.1

**Figure 7.** 2D fingerprint plots of co-crystal III.**Figure 8.** Energy framework diagram for (a) electrostatic, (b) dispersion and (c) total interaction energy.

The energy framework calculations is estimated from a single-point molecular wavefunction at B3LYP/6-31G(d,p) basis set [54,55]. The interaction energies viz., electrostatic, polarization, dispersion, and repulsion, between the molecular pairs were calculated. The visualization of different interaction energies; Coulomb interaction energy (red), dispersion energy (green), and total interaction energy (blue) of the compound are shown in Figure 8. The cylinders in the energy framework represent the relative strengths of molecular packing in different directions. The molecular pair-wise interaction energies calculated for the construction of energy frameworks are used to evaluate the net interaction energies. The total interaction energies for electrostatic, polarization, dispersion and repulsion are -124.8, -29.1, -16.5, and 147.8 kJ/mol, respectively. The total energy is -76.5 kJ/mol.

#### 4. Conclusions

A supramolecular compound with different topologies has been prepared and structurally characterized. Single crystal X-ray diffraction studies led to unambiguous structure determination. The different hydrogen bond interaction modes led to stabilization and formation of co-crystals. Hydrogen bonds are viewed as the strongest and most directional of the intermolecular interactions which play an incomparable role in the formation of supramolecular structure. The dihedral angle between aminobenzothiazol and fluorobenzoic acid moieties is 170.78(8)°. Hirshfeld surface analysis was done to quantify and identify the robust synthons and to understand the overall packing pattern of the co-crystal.

#### Acknowledgements

Vivek Kumar Gupta is thankful to University of Jammu, Jammu, India, for financial support under Rashtriya Uchcharat Shiksha Abhiyan (RUSA) 2.0 Project. (Ref. No: RUSA/JU/2/2019-20/111/3588-3636). Bubun Banerjee is grateful to Akal University for financial assistance.

#### Supporting information

CCDC-1983312 contains the supplementary crystallographic data for this paper. These data can be obtained free of charge via <https://www.ccdc.cam.ac.uk/structures/>, or by e-mailing [data\\_request@ccdc.cam.ac.uk](mailto:data_request@ccdc.cam.ac.uk), or by contacting The Cambridge Crystallographic Data Centre, 12 Union Road, Cambridge CB2 1EZ, UK; fax: +44(0)1223-336033.

#### Disclosure statement

Conflict of interest: The authors declare that they have no conflict of interest. Ethical approval: All ethical guidelines have been adhered. Sample availability: Samples of the compounds are available from the author.

#### CRedit authorship contribution statement

Conceptualization: Vivek Kumar Gupta, Bubun Banerjee; Methodology: Bubun Banerjee, Varun Sharma; Software: Varun Sharma, Aditi Sharma; Validation: Vivek Kumar Gupta, Bubun Banerjee; Formal Analysis: Gurpreet Kaur, Varun Sharma; Investigation: Bubun Banerjee, Varun Sharma; Resources: Vivek Kumar Gupta, Bubun Banerjee; Data Curation: Varun Sharma, Aditi Sharma, Gurpreet Kaur; Writing - Original Draft: Bubun Banerjee, Varun Sharma; Writing - Review and Editing: Bubun Banerjee, Vivek Kumar Gupta; Visualization: Bubun Banerjee, Vivek Kumar Gupta; Funding acquisition: Vivek Kumar Gupta, Bubun Banerjee; Supervision: Vivek Kumar Gupta, Bubun Banerjee; Project Administration: Vivek Kumar Gupta, Bubun Banerjee.

#### ORCID and Email

Bubun Banerjee

 [banerjeebubun@gmail.com](mailto:banerjeebubun@gmail.com)

 <https://orcid.org/0000-0001-7119-9377>

Varun Sharma

 [varunsharma5228@gmail.com](mailto:varunsharma5228@gmail.com)

 <https://orcid.org/0000-0003-2866-8638>

Aditi Sharma

 [aditi2195sharma@gmail.com](mailto:aditi2195sharma@gmail.com)

 <https://orcid.org/0000-0001-7777-0896>

Gurpreet Kaur

 [kaur80328@gmail.com](mailto:kaur80328@gmail.com)

 <https://orcid.org/0000-0002-9685-7927>

Vivek Kumar Gupta

 [vivek.gupta2k9@gmail.com](mailto:vivek.gupta2k9@gmail.com)

 <https://orcid.org/0000-0003-2471-5943>

#### References

- Hong, Y.-L.; Manjunatha Reddy, G. N.; Nishiyama, Y. Selective detection of active pharmaceutical ingredients in tablet formulations using solid-state NMR spectroscopy. *Solid State Nucl. Magn. Reson.* **2020**, *106*, 101651.
- Curatolo, W. Physical chemical properties of oral drug candidates in the discovery and exploratory development settings. *Pharm. Sci. Technol. Today* **1998**, *1*, 387–393.
- Childs, S. L.; Chyall, L. J.; Dunlap, J. T.; Smolenskaya, V. N.; Stahly, B. C.; Stahly, G. P. Crystal engineering approach to forming cocrystals of amine hydrochlorides with organic acids. Molecular complexes of fluoxetine hydrochloride with benzoic, succinic, and fumaric acids. *J. Am. Chem. Soc.* **2004**, *126*, 13335–13342.
- Schmidt, J.; Snipes, W. Free radical formation in a gamma-irradiated pyrimidine-purine co-crystal complex. *Int. J. Radiat. Biol. Relat. Stud. Phys. Chem. Med.* **1967**, *13*, 101–109.
- Etter, M. C. Hydrogen bonds as design elements in organic chemistry. *J. Phys. Chem.* **1991**, *95*, 4601–4610.
- Panunto, T. W.; Urbanczyk-Lipkowska, Z.; Johnson, R.; Etter, M. C. Hydrogen-bond formation in nitroanilines: the first step in designing acentric materials. *J. Am. Chem. Soc.* **1987**, *109*, 7786–7797.
- Etter, M. C.; Urbanczyk-Lipkowska, Z.; Zia-Ebrahimi, M.; Panunto, T. W. Hydrogen bond-directed cocrystallization and molecular recognition properties of diarylureas. *J. Am. Chem. Soc.* **1990**, *112*, 8415–8426.
- Etter, M. C.; Reutzel, S. M.; Choo, C. G. Self-organization of adenine and thymine in the solid state. *J. Am. Chem. Soc.* **1993**, *115*, 4411–4412.
- Vishweshwar, P.; McMahon, J. A.; Bis, J. A.; Zaworotko, M. J. Pharmaceutical co-crystals. *J. Pharm. Sci.* **2006**, *95*, 499–516.
- Jayasankar, A.; Somwangthanaroj, A.; Shao, Z. J.; Rodríguez-Hornedo, N. Cocrystal formation during cogrinding and storage is mediated by amorphous phase. *Pharm. Res.* **2006**, *23*, 2381–2392.
- Sokolov, A. N.; Frisci, T.; MacGillivray, L. R. Enforced face-to-face stacking of organic semiconductor building blocks within hydrogen-bonded molecular cocrystals. *J. Am. Chem. Soc.* **2006**, *128*, 2806–2807.
- Papaefstathiou, G. S.; Zhong, Z.; Geng, L.; MacGillivray, L. R. Coordination-driven self-assembly directs a single-crystal-to-single-crystal transformation that exhibits photocontrolled fluorescence. *J. Am. Chem. Soc.* **2004**, *126*, 9158–9159.
- Cheney, M. L.; McManus, G. J.; Perman, J. A.; Wang, Z.; Zaworotko, M. J. The role of cocrystals in solid-state synthesis: Cocrystal-controlled solid-state synthesis of imides. *Cryst. Growth Des.* **2007**, *7*, 616–617.
- Friščić, T.; MacGillivray, L. R. Reversing the code of a template-directed solid-state synthesis: a bipyridine template that directs a single-crystal-to-single-crystal [2 + 2] photodimerisation of a dicarboxylic acid. *Chem. Commun. (Camb.)* **2005**, 5748–5750.
- Kim, J. H.; Lindeman, S. V.; Kochi, J. K. Charge-transfer forces in the self-assembly of heteromolecular reactive solids: successful design of unique (single-crystal-to-single-crystal) Diels–Alder cycloadditions. *J. Am. Chem. Soc.* **2001**, *123*, 4951–4959.
- Gao, X.; Frisci, T.; MacGillivray, L. R. Supramolecular construction of molecular ladders in the solid state. *Angew. Chem. Int. Ed Engl.* **2004**, *43*, 232–236.
- Al-Tel, T. H.; Al-Qawasmeh, R. A.; Zaarour, R. Design, synthesis and in vitro antimicrobial evaluation of novel Imidazo[1,2-a]pyridine and imidazo[2,1-b][1,3]benzothiazole motifs. *Eur. J. Med. Chem.* **2011**, *46*, 1874–1881.
- Lee, Y.-R.; Jin, G. H.; Lee, S.-M.; Park, J.-W.; Ryu, J.-H.; Jeon, R.; Park, B.-H. Inhibition of TNF- $\alpha$ -mediated inflammatory responses by a benzodioxolylacetyl-amino-linked benzothiazole analog in human fibroblast-like synoviocytes. *Biochem. Biophys. Res. Commun.* **2011**, *408*, 625–629.
- Kamal, A.; Srikanth, Y. V. V.; Naseer Ahmed Khan, M.; Ashraf, M.; Kashi Reddy, M.; Sultana, F.; Kaur, T.; Chashoo, G.; Suri, N.; Sehar, I.; Wani, Z. A.; Saxena, A.; Sharma, P. R.; Bhushan, S.; Mondhe, D. M.; Saxena, A. K. 2-Anilino nicotinyln linked 2-aminobenzothiazoles and [1,2,4]triazolo

- [1,5-b] [1,2,4]benzothiadiazine conjugates as potential mitochondrial apoptotic inducers. *Bioorg. Med. Chem.* **2011**, *19*, 7136–7150.
- [20]. Kamal, A.; Reddy, K. S.; Khan, M. N. A.; Shetti, R. V. C. R. N. C.; Ramaiah, M. J.; Pushpavalli, S. N. C. V. L.; Srinivas, C.; Pal-Bhadra, M.; Chourasia, M.; Sastry, G. N.; Juvekar, A.; Zingde, S.; Barkume, M. Synthesis, DNA-binding ability and anticancer activity of benzothiazole/benzoxazole-pyrrolo[2,1-c][1,4]benzodiazepine conjugates. *Bioorg. Med. Chem.* **2010**, *18*, 4747–4761.
- [21]. Choi, M.-M.; Kim, E.-A.; Hahn, H.-G.; Nam, K. D.; Yang, S.-J.; Choi, S. Y.; Kim, T. U.; Cho, S.-W.; Huh, J.-W. Protective effect of benzothiazole derivative KHG21834 on amyloid beta-induced neurotoxicity in PC12 cells and cortical and mesencephalic neurons. *Toxicology* **2007**, *239*, 156–166.
- [22]. Sharma, P. C.; Sinhar, A.; Sharma, A.; Rajak, H.; Pathak, D. P. Medicinal significance of benzothiazole scaffold: an insight view. *J. Enzyme Inhib. Med. Chem.* **2013**, *28*, 240–266.
- [23]. Deng, X.-Q.; Song, M.-X.; Wei, C.-X.; Li, F.-N.; Quan, Z.-S. Synthesis and anticonvulsant activity of 7-alkoxy-triazolo-[3,4-b]benzo[d]thiazoles. *Med. Chem.* **2010**, *6*, 313–320.
- [24]. Jimonet, P.; Audiau, F.; Barreau, M.; Blanchard, J. C.; Boireau, A.; Bour, Y.; Coléno, M. A.; Doble, A.; Doerflinger, G.; Huu, C. D.; Donat, M. H.; Duchesne, J. M.; Ganil, P.; Guérémy, C.; Honor, E.; Just, B.; Kerphirique, R.; Gontier, S.; Hubert, P.; Laduron, P. M.; Le Blevic, J.; Meunier, M.; Miquet, J. M.; Nemecek, C.; Mignani, S. Riluzole series. Synthesis and in vivo “antiglutamate” activity of 6-substituted-2-benzothiazolamines and 3-substituted-2-imino-benzothiazolines. *J. Med. Chem.* **1999**, *42*, 2828–2843.
- [25]. Bowyer, P. W.; Gunaratne, R. S.; Grainger, M.; Withers-Martinez, C.; Wickramasinghe, S. R.; Tate, E. W.; Leatherbarrow, R. J.; Brown, K. A.; Holder, A. A.; Smith, D. F. Molecules incorporating a benzothiazole core scaffold inhibit the N-myristoyltransferase of Plasmodium falciparum. *Biochem. J.* **2007**, *408*, 173–180.
- [26]. Huang, Q.; Mao, J.; Wan, B.; Wang, Y.; Brun, R.; Franzblau, S. G.; Kozikowski, A. P. Searching for new cures for tuberculosis: design, synthesis, and biological evaluation of 2-methylbenzothiazoles. *J. Med. Chem.* **2009**, *52*, 6757–6767.
- [27]. Kaur, G.; Moudgil, R.; Shamim, M.; Gupta, V. K.; Banerjee, B. Camphor sulfonic acid catalyzed a simple, facile, and general method for the synthesis of 2-arylbenzothiazoles, 2-arylbenzimidazoles, and 3H-spiro[benzo[d]thiazole-2,3'-indolin]-2'-ones at room temperature. *Synth. Commun.* **2021**, *51*, 1100–1120.
- [28]. Sharma, V.; Kaur, G.; Singh, A.; Banerjee, B.; Gupta, V. K. Synthesis and characterization of 2-aminobenzothiazol and 1-methylisatin co-Crystal. *Crystallogr. Rep.* **2020**, *65*, 1195–1201.
- [29]. Sharma, V.; Karmakar, R.; Brahmachari, G.; Gupta, V. K. Synthesis, spectroscopic characterization, crystal structure, theoretical (DFT) studies and molecular docking analysis of biologically potent isopropyl 5-chloro-2-hydroxy-3-oxo-2,3-dihydrobenzofuran-2-carboxylate. *Mol. Cryst. Liq. Cryst.* **2022**, *1*–22.
- [30]. Sharma, V.; Slathia, N.; Mahajan, S.; Kapoor, K. K.; Gupta, V. K. Synthesis, characterization, crystal structure, molecular docking analysis and other physico-chemical properties of (E)-2-(3,4-dimethoxystyryl)quinoline. *Polycycl. Aromat. Compd.* **2021**, *1*–25.
- [31]. Kaur, G.; Singh, A.; Bala, K.; Devi, M.; Kumari, A.; Devi, S.; Devi, R.; Gupta, V. K.; Banerjee, B. Naturally occurring organic acid-catalyzed facile diastereoselective synthesis of biologically active (E)-3-(arylimino)indolin-2-one derivatives in water at room temperature. *Curr. Org. Chem.* **2019**, *23*, 1778–1788.
- [32]. Sharma, P.; Subbulakshmi, K. N.; Narayana, B.; Sarojini, B. K.; Kant, R. Crystal structure of 2-(thiophen-2-yl)-1-(5-thioxo-4,5-dihydro-1,3,4-oxadiazol-2-yl)ethenyl]benzamide : N,N-dimethylformamide (1 : 1). *Crystallogr. Rep.* **2016**, *61*, 230–233.
- [33]. Sharma, A.; Nurjamil, K.; Banerjee, B.; Brahmachari, G.; Gupta, V. K. Synthesis, characterization, and crystal structure of 5'-amino-4,4'-dichloro-2'-Nitro-2',3'-dihydro-[1,1':3,1''-terphenyl]-4',4',6'([1'H]-tricarbanitrile-dimethyl sulfoxide. *Crystallogr. Rep.* **2020**, *65*, 1208–1211.
- [34]. Sharma, V.; Banerjee, B.; Sharma, A.; Gupta, V. K. Synthesis, X-ray crystal structure, Hirshfeld surface analysis, and molecular docking studies of DMSO/H<sub>2</sub>O solvate of 5-chlorospiro[indoline-3,7'-pyrano[3,2-c:5,6-c']dichromene]-2,6',8'-trione. *Eur. J. Chem.* **2021**, *12*, 382–388.
- [35]. Sharma, V.; Banerjee, B.; Kaur, G.; Gupta, V. K. X-ray crystal structure analysis of 5-bromospiro[indoline-3,7'-pyrano[3,2-C:5,6-C']dichromene]-2,6',8'-trione. *Eur. J. Chem.* **2021**, *12*, 187–191.
- [36]. Sharma, N.; Brahmachari, G.; Banerjee, B.; Kant, R.; Gupta, V. K. 6-Amino-3-methyl-4-(3,4,5-tri-meth-oxy-phen-yl)-2,4-di-hydro-pyrano [2,3-c]pyrazole-5-carbo-nitrile. *Acta Crystallogr. Sect. E Struct. Rep. Online* **2014**, *70*, o875-6.
- [37]. Kaur, G.; Shamim, M.; Bhardwaj, V.; Gupta, V. K.; Banerjee, B. Mandelic acid catalyzed one-pot three-component synthesis of  $\alpha$ -aminonitriles and  $\alpha$ -aminophosphonates under solvent-free conditions at room temperature. *Synth. Commun.* **2020**, *50*, 1545–1560.
- [38]. Sharma, N.; Brahmachari, G.; Banerjee, B.; Kant, R.; Gupta, V. K. Ethyl 6-amino-5-cyano-4-phenyl-2,4-di-hydro-pyrano[2,3-c]pyrazole-3-carboxyl-ate dimethyl sulfoxide monosolvate. *Acta Crystallogr. Sect. E Struct. Rep. Online* **2014**, *70*, o795-6.
- [39]. Singh, A.; Kaur, G.; Kaur, A.; Gupta, V. K.; Banerjee, B. A general method for the synthesis of 3,3-bis(indol-3-yl)indolin-2-ones, bis(indol-3-yl)(aryl)methanes and tris(indol-3-yl)methanes using naturally occurring mandelic acid as an efficient organo-catalyst in aqueous ethanol at room temperature. *Curr. Green Chem.* **2020**, *7*, 128–140.
- [40]. Kaur, G.; Kumar, R.; Saroch, S.; Gupta, V. K.; Banerjee, B. Mandelic acid: An efficient organo-catalyst for the synthesis of 3-substituted-3-hydroxy-indolin-2-ones and related derivatives in aqueous ethanol at room temperature. *Curr. organocatalysis* **2021**, *8*, 147–159.
- [41]. Sheldrick, G. M. Crystal structure refinement with SHELXL. *Acta Crystallogr. C Struct. Chem.* **2015**, *71*, 3–8.
- [42]. Farrugia, L. J. WinGX and ORTEP for Windows: an update. *J. Appl. Crystallogr.* **2012**, *45*, 849–854.
- [43]. Nardelli, M. PARST95 – an update to PARST: a system of Fortran routines for calculating molecular structure parameters from the results of crystal structure analyses. *J. Appl. Crystallogr.* **1995**, *28*, 659–659.
- [44]. Spek, A. L. Structure validation in chemical crystallography. *Acta Crystallogr. D Biol. Crystallogr.* **2009**, *65*, 148–155.
- [45]. Spackman, P. R.; Turner, M. J.; McKinnon, J. J.; Wolff, S. K.; Grimwood, D. J.; Jayatilaka, D.; Spackman, M. A. CrystalExplorer: a program for Hirshfeld surface analysis, visualization and quantitative analysis of molecular crystals. *J. Appl. Crystallogr.* **2021**, *54*, 1006–1011.
- [46]. Farrugia, L. J. ORTEP-3 for Windows – a version of ORTEP-III with a Graphical User Interface (GUI). *J. Appl. Crystallogr.* **1997**, *30*, 565–565.
- [47]. Allen, F. H.; Kennard, O.; Watson, D. G.; Brammer, L.; Guy Orpen, A.; Taylor, R. Tables of bond lengths determined by X-ray and neutron diffraction. Part 1. Bond lengths in organic compounds. *J. Chem. Soc. Perkin Trans. 2* **1987**, S1–S19.
- [48]. Jin, S.; Yan, P.; Wang, D.; Xu, Y.; Jiang, Y.; Hu, L. Salt and co-crystal formation from 6-bromobenzo[d]thiazol-2-amine and different carboxylic acid derivatives. *J. Mol. Struct.* **2012**, *1016*, 55–63.
- [49]. Colapietro, M.; Domenicano, A.; Pela Ceccarini, G. Structural studies of benzene derivatives. V. The crystal and molecular structure of p-fluorobenzoic acid. *Acta Crystallogr. B* **1979**, *35*, 890–894.
- [50]. Bernstein, J.; Davis, R. E.; Shimoni, L.; Chang, N.-L. Patterns in hydrogen bonding: Functionality and graph set analysis in crystals. *Angew. Chem. Int. Ed. Engl.* **1995**, *34*, 1555–1573.
- [51]. Spackman, M. A.; Jayatilaka, D. Hirshfeld surface analysis. *CrystEngComm* **2009**, *11*, 19–32.
- [52]. Hoffmann *Solids and surfaces - a chemist's view of bonding in extended structures*; John Wiley & Sons: Milton, QLD, Australia, 1989.
- [53]. McKinnon, J. J.; Mitchell, A. S.; Spackman, M. A. Hirshfeld surfaces: A new tool for visualising and exploring molecular crystals. *Chemistry* **1998**, *4*, 2136–2141.
- [54]. Edwards, A. J.; Mackenzie, C. F.; Spackman, P. R.; Jayatilaka, D.; Spackman, M. A. Intermolecular interactions in molecular crystals: what's in a name? *Faraday Discuss.* **2017**, *203*, 93–112.
- [55]. Mackenzie, C. F.; Spackman, P. R.; Jayatilaka, D.; Spackman, M. A. CrystalExplorer model energies and energy frameworks: extension to metal coordination compounds, organic salts, solvates and open-shell systems. *IUCr* **2017**, *4*, 575–587.



Copyright © 2022 by Authors. This work is published and licensed by Atlanta Publishing House LLC, Atlanta, GA, USA. The full terms of this license are available at <http://www.eurjchem.com/index.php/eurjchem/pages/view/terms> and incorporate the Creative Commons Attribution-Non Commercial (CC BY NC) (International, v4.0) License (<http://creativecommons.org/licenses/by-nc/4.0>). By accessing the work, you hereby accept the Terms. This is an open access article distributed under the terms and conditions of the CC BY NC License, which permits unrestricted non-commercial use, distribution, and reproduction in any medium, provided the original work is properly cited without any further permission from Atlanta Publishing House LLC (European Journal of Chemistry). No use, distribution or reproduction is permitted which does not comply with these terms. Permissions for commercial use of this work beyond the scope of the License (<http://www.eurjchem.com/index.php/eurjchem/pages/view/terms>) are administered by Atlanta Publishing House LLC (European Journal of Chemistry).